Chapter 12

The Fast Muon Kicker

Injected muons exit the downstream end of the inflector magnet, and enter the good field region of the main dipole. The trajectory of the muons exiting the inflector is a circle displaced 77 mm radially from the closed orbit of the storage ring. The muons emerge from the inflector into the full 1.41T field of the dipole but with trajectories that are on average, tangential to the displaced circle. The muons cross the closed orbit of the storage ring, that is the orbit at the magic radius, about 90° azimuthally around the ring from the end of the inflector. As shown in Fig. 12.1, The muons intersect the closed (ideal) orbit at an angle of $\theta_0 = 10.8$mrad. The minimum crossing angle, namely $\theta_0 = 10.8$mrad obtains for trajectories that are tangential at the inflector exit. Any angle, positive or negative, with respect to the tangent line results in crossing angle greater than the minimum.
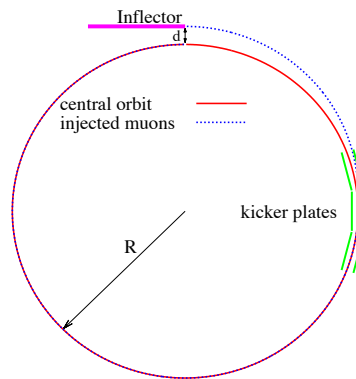
Figure 12.1: Muons exit the inflector displaced $d = 77$mm from the central orbit and cross the central orbit at an angle of 10.8 mrad 90 degrees around the ring. The 10.8mrad kick directs muons onto the central orbit.

Simulation of the injection of a distribution of muons that includes scattering in the inflector coil ends, and scattering in the quadrupole plate indicates that the total kick angle that achieves maximum storage efficiency is 10.8 ± 0.4 mrad. Our target for the kicker system

is a 12.8 mrad kick, so that there is sufficient operating margin, and in anticipation of a new larger aperture inflector that would displace the center of the inflector aperture further from the magic radius.

The fast kicker is a pulsed magnet with vertical field that directs the muons onto the ideal orbit, by compensating the crossing angle. Ideally, the centroid of the injected bunch, on exiting the field of the kicker plates, will coincide with the closed orbit of the storage ring, thus eliminating residual coherent betatron oscillation. The 10.8 - 12.8 mrad kick corresponds to an integrated vertical field of 1.1 - 1.3 kG-m.

The E989 kicker will be comprised of three independent 1.27m long magnets, each with a dedicated pulse forming network as current generator. Muons are delivered to the storage ring in pulses with 95% transverse emittance near 40π mm-mrad, pulse length of about 120ns and at a peak repitition rate 100Hz and an average rate of 12Hz. The ideal kicker field maintains a flat top at the required 285 - 336 Gauss, for the full 120ns, and then returns to zero before the lead muons complete a single revolution and re-enter the kicker aperture 149ns later. (The revolution period of the ring is 149 ns). The rise and fall time of the kicker pulse is ultimately determined by the finite length, and transit time of the pulse in each of the three strip line magnets. Faster rise and fall obtains with shorter magnets.

The injection of muons into the storage ring is complicated by several requirements:

1. Since the magnet is continuous, any kicker device has to be inside of the precision magnetic field region.

2. The kicker hardware cannot contain magnetic elements such as ferrites, since they will spoil the uniform magnetic field.

3. Any eddy currents produced in the vacuum chamber, or in the kicker electrodes, must be negligible by 10 to 20 μs after injection, or must be well known and corrected for in the measurement.

4. Any kicker magnet hardware must fit within the real estate occupied by the E821 kicker, which employed three 1.7 m long devices.

5. The kicker pulse should be shorter than the cyclotron period of 149 ns

12.1   Requirements for the E989 Kicker

The need for a fast muon kicker was introduced in Section 3.2. Direct muon injection was the key factor that enabled E821 to accumulate 200 times the data as the preceeding CERN experiment. Since E989 needs more than twenty times as much data as E821, it is critical that the limitations of the E821 kicker be mitigated. The layout of the E821 storage ring is shown in Fig 12.2. The three kicker magnets are located approximately 1/4 of a betatron wavelength around from the inflector exit.
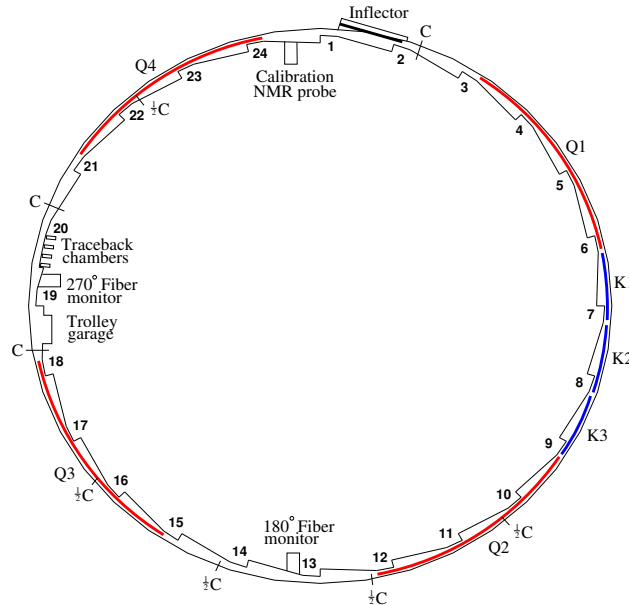
Figure 12.2: The layout of the storage ring, as seen from above, showing the location of the inflector, the kicker sections (labeled K1-K3), and the quadrupoles (labeled Q1-Q4).

12.1.1   The E821 Kicker and its Limitations

The E821 kicker [1] consisted of three identical sectors with 1.7 m long parallel plates carrying current in opposite directions, located as shown in Fig. 12.2. Each section was powered by a pulse forming network where a HV capacitor was resonantly charged to $\simeq$ 95 kV, and then shorted to ground by a deuterium thyratron, giving a characteristic damped LCR oscillating current and magnetic field. The resulting LCR pulse is shown in Fig. 12.3(Left). The LCR pulse was much wider than the muon pulse length, in fact significantly longer than the cyclotron period of 149 ns. This is emphasized by the series of red gaussians which are separated by the 149 ns revolution period. Thus the beam is kicked several times before the LCR pulse dies away. Simulations show that the peak field achieved with the LCR pulser was only 120G and yielded a kick angle of barely 6 mrad. Thanks to the multi-turn width of the pulse, the cumulative kick was sufficient to store muons.

The kicker units began sparking around 95 kV, limiting the pulse current. The number of muons stored vs. kicker high voltage in the E821 experiment is shown in Fig. 12.3(Right). At the maximum accessible voltage, the number of stored muons had not yet plateaued. It is not entirely clear how many muons might have been stored if it had been possible to increase the voltage until the maximum number of stored muons was reached. Simulations suggest that the number stored would have increased by 30%. But even had that higher capture efficiency been reached, there would have remained a significant coherent betatron oscillation do to the temporal nonuniformity of the kick over the length of the muon pulse.
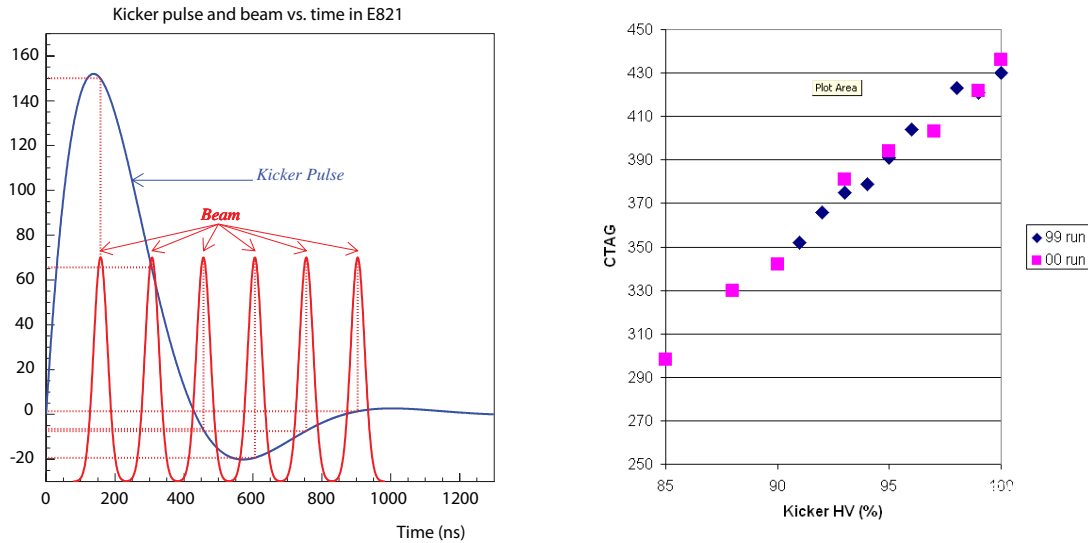
Figure 12.3: (Left)The E821 kicker LCR waveform (blue). The red pulses represent the injected beam, which has a cyclotron period of 149 ns. (Right) The number of stored muons versus kicker high voltage (arbitrary units).

12.2   New Kicker Design

The design of the kicker for E989 attempts to address the shortcomings of the E821 kicker, specifically with respect to the pulse shape and pulse amplitude. The E989 pulse forming network is based on a Blumlein triaxial transmission line as an alternative to the E821 LCR PFN. The kicker plates are redesigned with somewhat higher efficiency, that is, higher magnetic field between the plates per unit current through the plates. Fig. 12.4 is a rendering of the 1.27 m long plates of the new kicker magnets along with hardware for mounting the plates in the vacuum chamber and the tracks for the NMR trolley.

The E989 current generator is a variation on a transmission line PFN. Consider each 1.27 m long pair of kicker plates a transmission line with impedance Z_L, and imagine, at least conceptually, that each is terminated with a resistive load $R = Z_L$. If the impedance of the PFN transmission line matches the impedance of kicker plates and load, then the current pulse will have width $\tau = 2L/c$ where L and c are the length and group velocity of the PFN, and peak current $I = V/Z$, where V and Z are the peak charging voltage and the impedance of the line respectively. Then the rise time of the pulse is limited only by the switching time of the thyratron of about 20-30ns.

The configuration with transmission line, kicker magnet, and load all in series, is however impractical in this application, because of the relatively high impedance of the kicker magnet plates. The estimated impedance of the kicker plates is nearly 600 Ω. As will be shown below, the current required to achieve the requisite $\sim$ 280 G field between the plates is about 4.7 kA. If the impedance of the PFN is matched to the impedance of the kicker plates, a charging voltage of nearly 2.8 MV would be required to push 4.7kA through the load. Such an arrangement would also require terminating the kicker plates with a resistor with result that
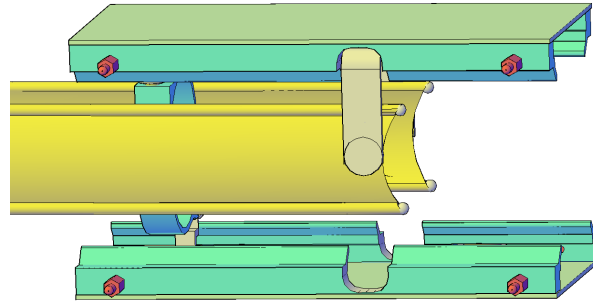
Figure 12.4: The kicker plates for E989. The current pulse is fed to the 1.27m long plates at the far end to the left of the plot. A jumper connecting the plates is placed at the near end that closes the circuit as shown. The plates are suspended from the top of the vacuum chamber. The NMR trolley rails are shown in green. The trolley will roll between the plates.

the plates would float to high voltage with each pulse.

12.2.1   Current source

Instead of terminating the kickers with a resistive load, the load resistor is placed between the pulse forming network and the kicker plates. The impedance of the PFN transmission line is simply matched to the load resistor. The load resistance, $R = 12.5\Omega$, is chosen so that the requisite charging voltage (V=IR=54kV) is well within reach of an available thyratron switch. The reflections that will inevitably arise from the imperfect match at the junction of load resistor and kicker plates, will be confined to the plates, and dissipated on the timescale of the plate round trip transit time of about 10ns. The triaxial line and matched terminating resistor act as a current source. At the transition through the load resistor to the kicker, the transmission line is tapered to near zero impedance. The configuration is then equivalent to a current source as there will be zero voltage at the end of the taper. A schematic of the power supply, charging circuit, Blumlein current generator (see next section) and kicker is shown in Fig. 12.5.

12.3   Blumlein Pulse Forming Network

The pulse forming network developed for the kicker is a Blumlein triaxial transmission line. The Blumlein is shown schematically in Fig. 12.6. The LCR circuit used in E821, and a coaxial transmission line are included in the Fig. 12.6 for comparison. The equivalent circuit for a Blumlein is a pair of series bi-axial lines with a shared conductor and it is so rendered in Fig. 12.7. The width of the pulse

$$\tau = \frac{2L}{v} = 2L\frac{\sqrt{\mu\epsilon}}{c}.$$
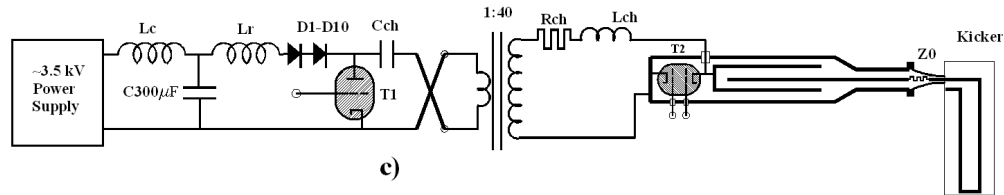
Figure 12.5: Schematic of the kicker, pulse forming network and charging circuit. The Blumlein, resistive load ($Z_0 = 12.5\Omega$) and kicker are in series to the right of the figure. In the final installation the load resistor is mounted near the vacuum chamber coupling directly to the kicker plates. The Blumlein connects to the resistor via high voltage coax.

For the bi-axial line the voltage at a matched load is half the charging voltage. For the Blumlein, output voltage and charging voltage are one and the same[2]. Another advantage of the Blumlein as compared to a bi-axial transmission line is that the base of the thyratron can be fixed at ground potential. A bi-axial pulse forming network would require that the base of the tube float to high voltage when the thyratron is switched.
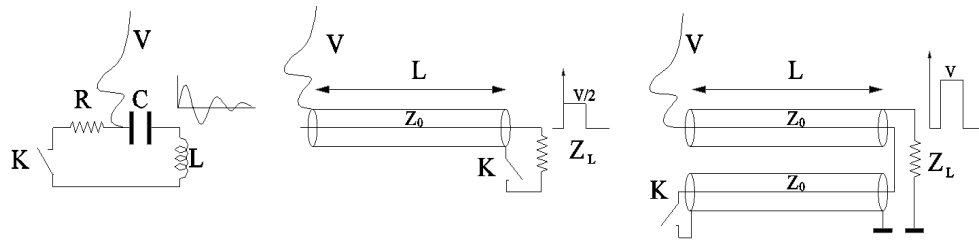
Figure 12.6: The overdamped LCR circuit at left was used in E821. The line labeled "V" indicates the charging voltage and K the thyratron switch. At center is a coaxial transmission line PFN. The Blumlein equivalent circuit is at the right. The corresponding pulse shape is shown for each of the configurations. Note that for both coaxial and triaxial lines, pulse width is proportional to twice the line length. Voltage across a matched load for the Blumlein is twice that of the coax. The Blumlein pulse is delayed by half of the pulse width.

The schematic of the 12.5Ω Blumlein prototype is shown in cross section in Fig. 12.8. The middle conductor is connected through a large resistance and inductance to the high voltage power supply. Current flows through the load Z_L from the central conductor during the charging cycle. The thyratron (T) shorts the middle conductor to the outer conductor and after a delay of $T/2$, where T is the width of the current pulse generated by the line, the current flows through the resistive load and into the kicker.

Some details of the Blumlein are shown in Fig. 12.9. The basic electrical properties of the pulser with an equivalent circuit are computed with SPICE. Each of the two series coaxial lines are modeled with discrete elements as shown in Fig. 12.10(Top). The kicker load is represented with characteristic capacitance and inductance. The current pulse through the kicker when the switch is closed, as computed with SPICE, is shown in Fig. 12.10(Bottom).
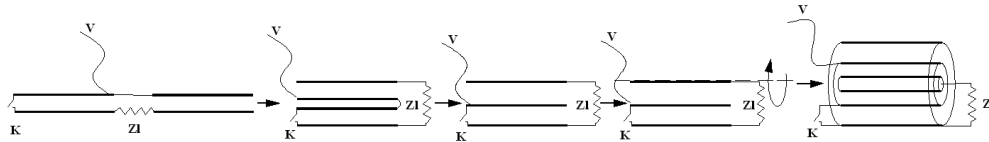
Figure 12.7: Topological modification of series coaxial lines into a tri-axial Blumlein transmission line. (One can choose the rotation axis coinciding with the lower plate).
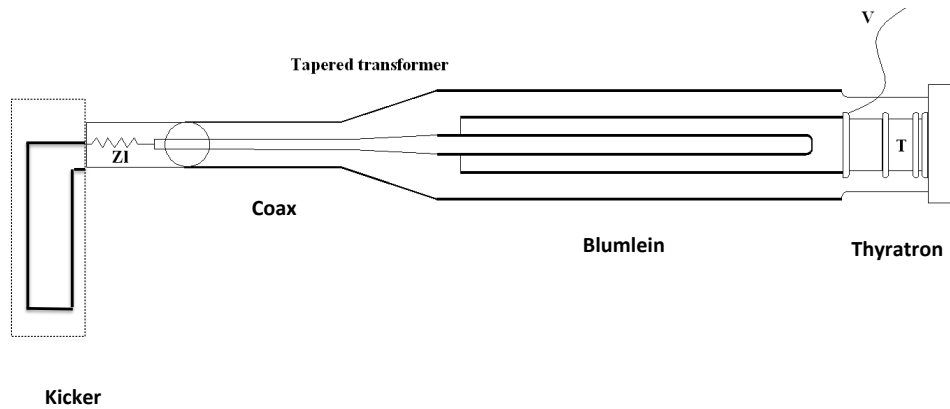
Figure 12.8: Middle conductor is charged to high voltage via the line labeled "V". The centermost conductor is coupled via a high voltage coaxial cable to the resistive load that is mounted directly to the input of the kicker. The thyratron (T) shorts the middle conductor to ground. The volumes between conductors, around the thyratron and load are all filled with transformer oil.

The impedance of the triaxial line is equivalent to the sum of the impedances of the series bi-axial lines. The middle conductor in Fig. 12.8 that is charged to high voltage serves as the inner conductor for one bi-axial line and the outer conductor for the other. The impedance of each of these bi-axial components is 6.25Ω. The output of the PFN is coupled to the load with four parallel 50Ω high voltage coaxial cables, with combined impedance of 12.5Ω. The blumlein and transition hardware is shown in Fig. 12.11.

A schematic of the Blumlein pulser connected via high voltage coax to the kicker inside the muon ring vacuum chamber is shown in Fig. 12.12. Also shown is the electronics rack with 1500 V power supply, thyratron driver, and thyratron trigger pulser. The cylindrical container sitting on the floor beside the rack is the oil tank with high voltage transformer. While the single high voltage transformer can in principle charge all three Blumleins for each of the three kickers, independent supplies will be deployed so that failures in the electronics of one PFN and kicker are not propagated to the others.
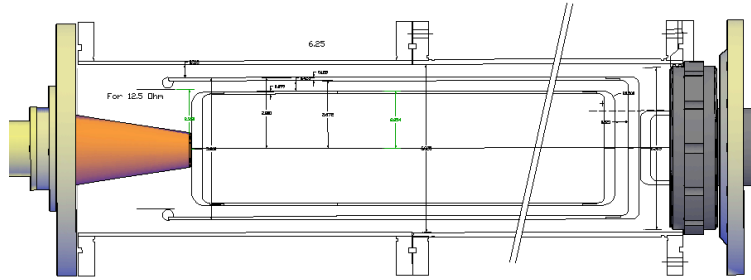
Figure 12.9: Cross section of 12.5Ω. Blumlein. The central conductor couples through the orange transition at the left of the figure to the load resistor and kicker. The middle conductor connects through the U bracket near the right to the thyratron (not shown). The penetration of the high voltage charging line through the outer conductor to the middle conductor is not shown.

12.3.1   Thyratron switch

A thyratron switch shorts the middle conductor of the Blumlein to ground, initiating the current pulse that drives the kicker. The peak current required to achieve the approximately 1.1 kG-m field depends on the cross sectional shape of the kicker plates (determining relationship between current and B-field), and plate length (limited to less than 5.1m). As will be shown in the next sections, a peak current in excess of 4kA is required. Table 12.1 summarizes the parameters of the kicker thyratron used in the E821 experiment and the high current two grid tube (thyratron model CX1725X[4]) that is used for the new kicker current generator.

Thyratron	CX1699 (E-821)	CX1725X
Peak Voltage [kV]	130	70
Peak Current [kA]	3	15
dI/dt [kA/μs]	10	<300
Repetition rate [Hz]	400	2000
Grids	4	2

Table 12.1: Evidently the E821 tube can not switch the requisite (>4kA) current. The CX1725X tube proposed for the new kicker pulse generator is faster (dI/dt), in addition to the higher current rating, and can more easily manage the repetition rate.
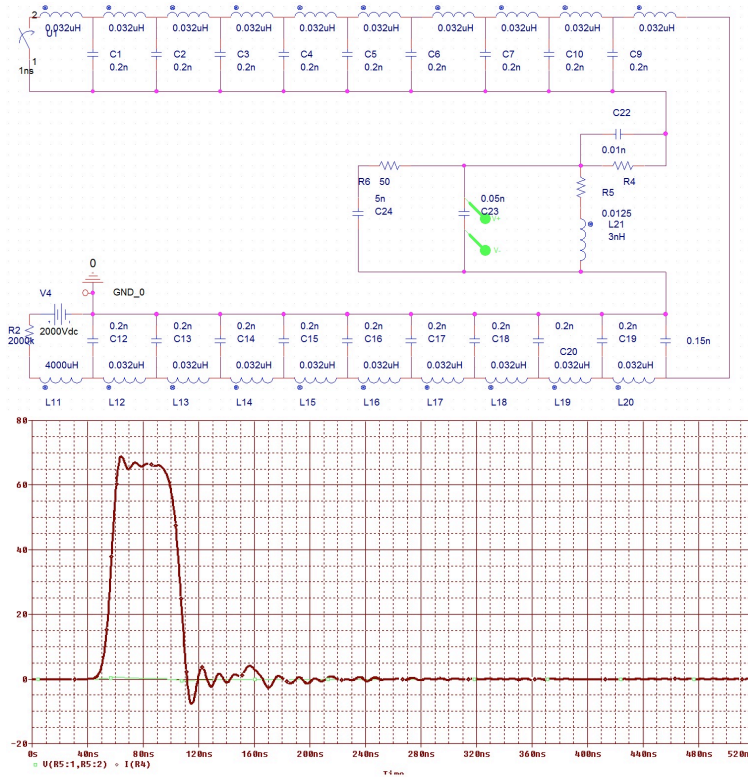
Figure 12.10: Discrete circuit element of the Blumlein that is shown as the right hand schematic in Fig. 12.6. Each of the two transmission lines is assembled with lumped inductance and capacitance. The kicker load is represented as inductance with small capacitance.

Note that in the Blumlein configuration, the thyratron current is twice the load current. The CX1725X can deliver up to 7500A to the load, well in excess of the anticipated requirement.

12.4   Kicker Plate Design

The geometry of the kicker plates is optimized for higher efficiency than the E821 design, that is higher midplane magnetic field for a given current through the plates. The field profile for the proposed plate geometry is shown in Fig. 12.13(Right) as compared to the E821 geometry in Fig. 12.13(Left). The calculation assumes a pulse width of 100ns and rise time of 20ns. As can be seen in Fig. 12.13, the E-821 plate geometry yields uniform vertical field over a larger region than the E-989 geometry, at the cost of significantly lower fields near the top and bottom edges of the plates. The advantage of the proposed E-989 geometry is that the field in the midplane is 65 Gauss for a plate current of 1000 A, as compared to
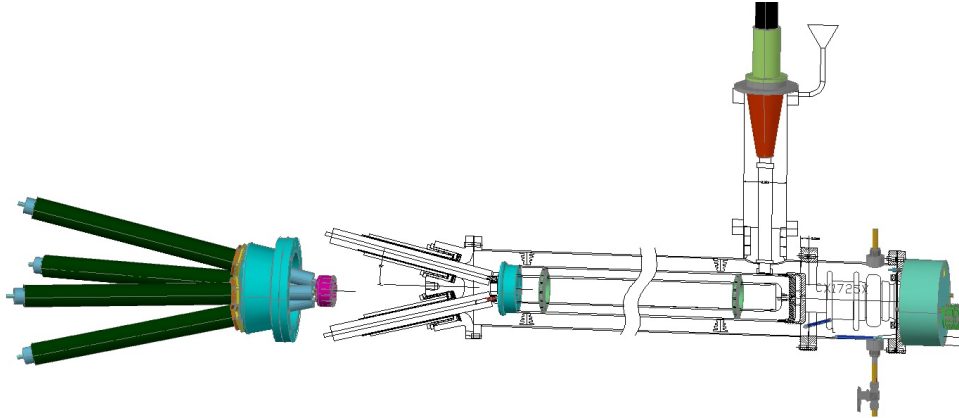
Figure 12.11: Transition from Blumlein (far right) to 4-50Ω cables. The 4 cables are coupled to the centermost conductor of the Blumlein. The high voltage charging transformer couples to the middle conductor via a feedthrough at the right. The thyratron switches the middle conductor to ground (outer conductor)

only 35 Gauss/kA for the E821 kicker magnet. The relative efficiencies of the two geometries corresponds to the ratio of the perimeters of the plates.

A full tracking simulation of the injection process shows that the somewhat weaker field away from the midplane in the E-989 geometry degrades capture efficiency by only a few percent. Also, by distancing the kicker plates from the vacuum chamber, long lived eddy currents induced in the aluminum chamber that might effect the local magnetic field are reduced.

12.4.1   Kicker Plate Length

There are 5.1m available in the storage ring for kicker plates. The required 10.8 to 12.8mrad kick corresponds to an integrated field of $1.11\mathrm{kG} - \mathrm{m} < \int \mathbf{B} \cdot d\mathbf{l} < 1.31\mathrm{kG} - \mathrm{m}$. Given the relation between B-field and peak current for the proposed plate geometry of 65G/kA the current requirement can be written $17\mathrm{kA} - \mathrm{m} < I_{peak}L < 20\mathrm{kA} - \mathrm{m}$. The rise and fall time of the current pulse depends on the length of the plates, and in particular increases with plate length. The peak current through the 12.5Ω resistive load is limited by the tube voltage maximum of 70kV to 5.6kA and therefore according to the inequality above the length L of the plates must be at least 3.6 m. In E989 there will be three, 1.27m long kickers corresponding to a total length of 3.8m, thus leaving a margin of about 10%. If the system is limited for any reason to $I < 5.6\mathrm{kA}$, there is space available in the storage ring for a fourth 1.27m long kicker. Note that in any event, the new kicker system will operate at voltage well below the $\sim 95\mathrm{kV}$ breakdown voltage of the E821 kickers.
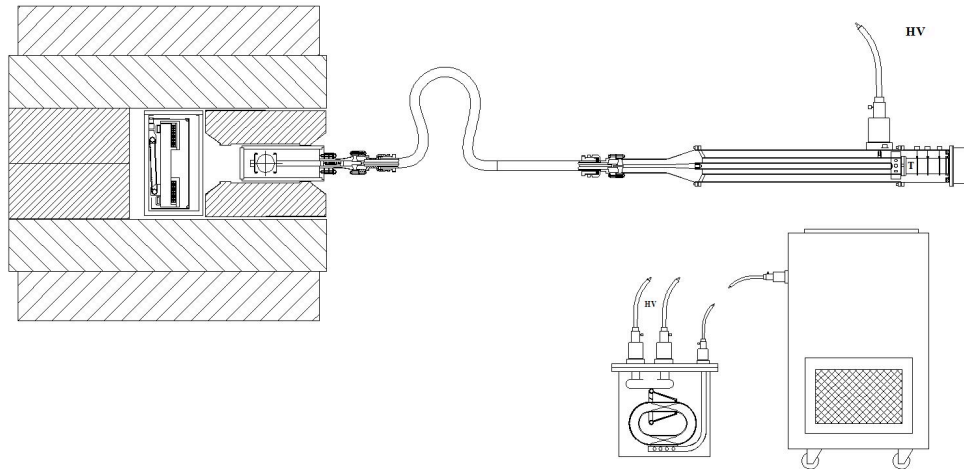
Figure 12.12: Blumlein is coupled through four parallel 50Ω high voltage coaxial cables to the kicker magnet inside the ring vacuum chamber. (Only a single coax is shown). High voltage power supply and thyratron driver are in the electronics rack at right. The 1:85 high voltage transformer that provides charging voltage to the PFN is in the oil tank to the left of the electronics rack.

12.4.2 Trolley rails

Whereas in the E821 configuration, the kicker plates served as rails for the NMR trolley, those functions will be separated in the new implementation as can be seen in Fig. 12.14. The NMR trolley will roll between the plates. The kicker plates will be suspended within a cage as shown in Fig. 12.15. Care will be taken to ensure the stability of the plates with respect to the time dependent forces associated with the current pulse. At the same time it is desireable to minimize the thickness of the plates so as to minimize scattering of decay electrons.

12.5 Kicker R&D at Cornell

A laboratory has been outfitted at Cornell to build and test a prototype Blumlein pulse forming network and fast kicker magnet. The electronics that has been recovered from the E821 experiment and re-assembled includes: high voltage power supply, high voltage charging transformer, and trigger pulser. Thyratron and driver were procured to match requirements of the new current generator and kicker plate geometry. The 9 meter long prototype 12.5Ω Blumlein is shown in Fig. 12.16,12.17 and 12.18. In order to maximize the pulse width the space between the concentric cylinders of the Blumlein is filled with castor oil with permittivity $\epsilon = 4.7$ (rather than the lower permittivity silicon oil). The vacuum chamber with prototype kicker plates is shown in the top left of Fig. 12.19(Left) and Fig. 12.20.

In order to better understand the dependence of pulse shape on kicker length (and kicker inductance), measurements were performed with kicker plates with different effective lengths.
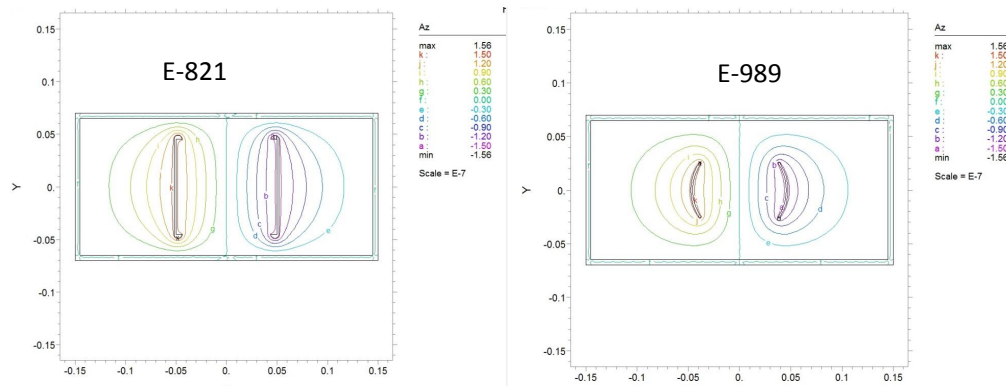
Figure 12.13: (Left) E821 kicker plate geometry and field lines computed with FLEX PDE. The boundary condition at the vacuum chamber surface includes the effect of induced currents due to fast rise time. Note the high density of field lines at the edge of the plate that also serves as the trolley rail. (Right) Proposed kicker plate geometry and magnetic field lines.

A photograph of the shorting bar used to change the effective plate length, and some of the measurements are shown in Fig. 12.19. The rise time clearly increases with the length of the kicker plates, indicating that the pulse shape is dominated by the properties of the load, rather than the thyratron switch. The length of the kicker plates is chosen so as to optimize the pulse shape consistent with the integrated field requirement and the peak current available from the pulse forming network. The optimimum length is 1.27 m (that is as short as is compatible with the available peak current). The Blumlein is coupled to the kicker using four 50Ω high voltage coaxial cables in parallel.

Three 12.5Ω Blumleins, each outfitted with the 2-gap CX1725X thyratron will drive three 127cm long kickers. If necessary, the rise and fall time of the current pulse can be made shorter by reducing the kicker length and the integrated field recovered by adding a fourth kicker (and Blumlein). With four kicker magnets, the 1.31kG-m integrated field could be achieved with magnet length of 90cm operating at 5146A.
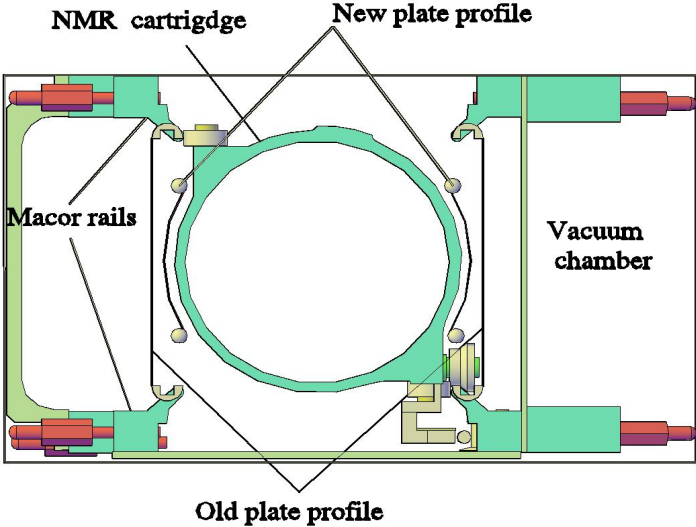
Figure 12.14: (Left)E821 kicker plates, new plates, NMR trolley, and new rails are all superimposed.
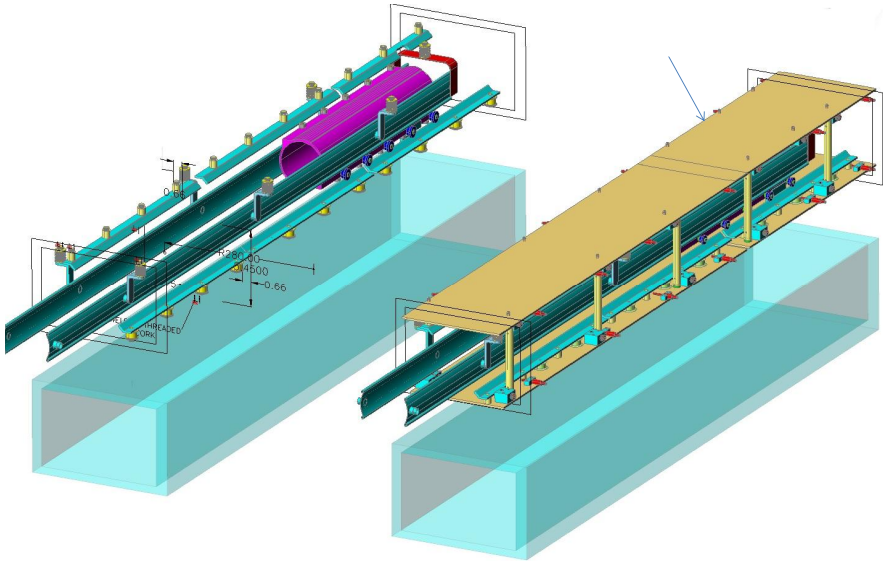
Figure 12.15: (Left)Plates suspended in cages with top and bottom of cage removed. (Right) Plates inside cages and outside of vacuum chamber below.

Figure 12.16: (Left) Blumlein. The black cable visible in the background couples the charging transformer to the middler conductor of the Blumlein. The thyratron is mounted horizontally inside the green cylinder at the far end. The space between the conductors of the Blumlein and the volume around the thyratron is filled with transformer oil. The central conductor of the Blumlein, that couples to the four coaxial cables is seen in the foreground. (Right) The fixture that will capture the four coaxial cables is mounted on the near end of the Blumlein.
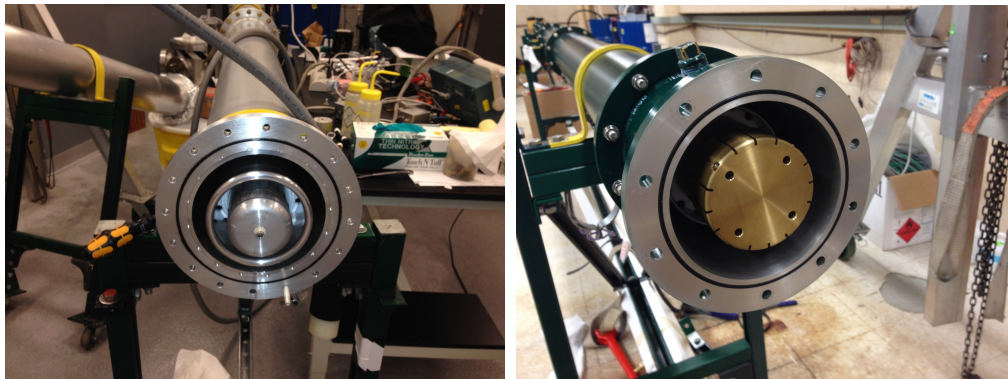
Figure 12.17: (Left) The three concentric cylinders of the Blumlein. The middle cylinder is charge to high voltage. The thyratron switch shorts the middle conductor to the outer cylinder. The current pulse propagates through the central conductor to the load. (Right) The central conductor with cap that couples to cables. The middle conductor is hidden from view.

Figure 12.18: (Left) Blumlein with thyratron end in background and transition to coax in foreground. Four parallel coaxial cables connect Blumlein to load resistor (shown in photograph at right) at vacuum chamber at left of photograph. (Right) The four coaxial cables from the Blumlein are coupled to four 50Ω resistors inside the cylindrical chamber. The downstream end of the resistors are coupled together and then to the kicker magnet inside the vacuum chamber at far right of photograph.
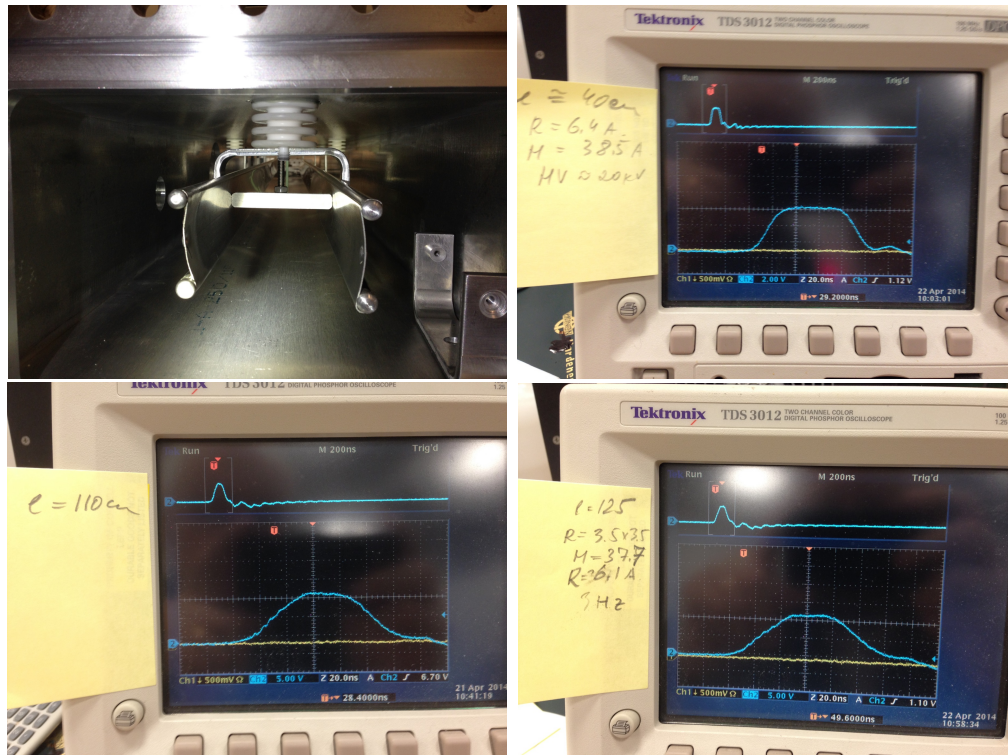
Figure 12.19: (Top left) Prototyper kicker plates with shorting bar. (Top right). Kicker magnetic field pulse measured with loop pickup with effective kicker length of 40cm. The time scale on the oscilloscope is 20ns/division. The rise and fall time of the pulse is 20ns, with a 50ns flat top. The total pulse length is consistent with the length of the Blumlein. (Bottom left) Magnetic field for 110cm kicker. (Bottom right) Magnetic field for 125cm kicker. The rise and fall time increase with the length of the kicker. The pulse shape is also observed to be sensitive to the thyratron reservoir current.)
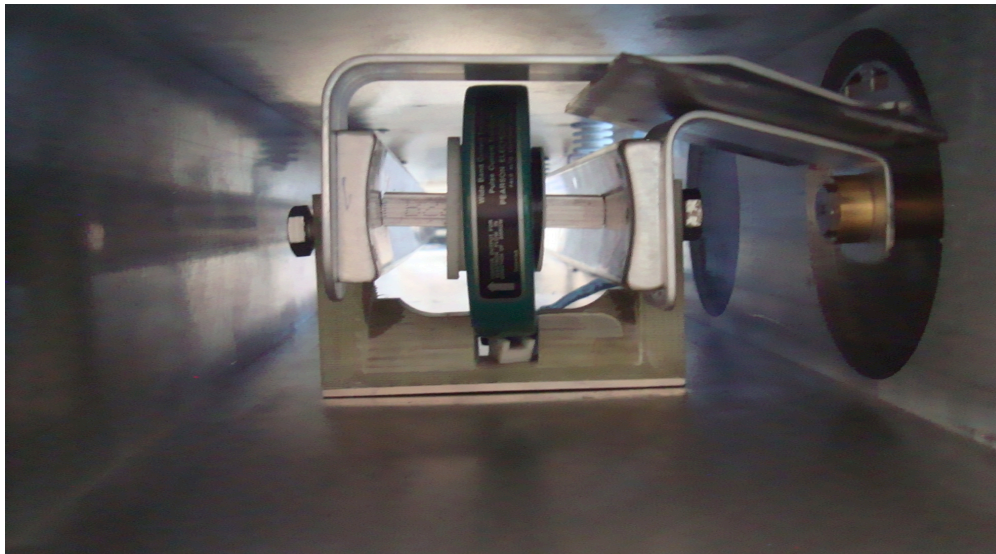
Figure 12.20: Kicker plates mounted in the vacuum chamber with couplings through chamber wall to 12.5Ω termination resistor. Here a current transformer is mounted on a shorting bar. The shorting bar can be moved along the length of the plates and the current measured as a function of plate length.
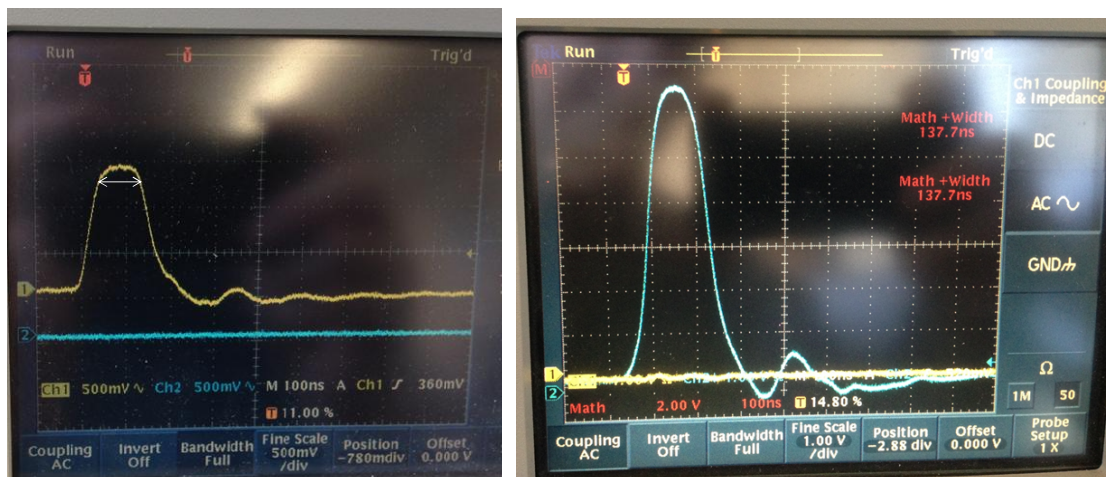
Figure 12.21: (Left)Current pulse with 35 cm plates. (Right) Current pulse with 127cm plates. Note that the rise and fall times are longer for the pulse at right and the flat top narrower. The tail that extends beyond 149 ns has negligible dependence on the length of the plates and is apparently due to mismatch of Blumlein, coax cable and load resistance.

12.6   Kicker Field Measurement

Measurement of the time dependent field of the kicker will ultimately determine the effectiveness of the design choices. Furthermore, it is essential to measure, and ideally eliminate, fields due to the eddy currents in the vacuum chamber and kicker plates, that are generated by the kicker pulse. If the eddy currents have a long decay time, any persistent field will introduce a systematic shift in a_μ.

A Faraday magnetometer has been designed and tested to measure the time dependence of the kicker field and associated persistent fields modeled on the device used in E821. The cylindrical TTG birefringent crystal is mounted in a G10 tube that passes through the vacuum chamber and between the kicker plates. Polarized light from the green laser mounted above the vacuum chamber, passes along the axis of the tube, through the crystal and then into a Wollaston prism that is mounted below the vacuum chamber as shown in Figure 12.22 and 12.23. The polarization direction of the light emerging from the crystal is rotated by an angle proportional to the magnetic field. The prism directs orthogonal polarizations into the two arms. The difference of the amplitude of the orthogonal components is a measure of the change in field. Ports machined in the prototype vacuum chamber transmit polarized laser light into the chamber and then through a birefringent crystal that is mounted between the plates in the laboratory as shown in Figure 12.24.
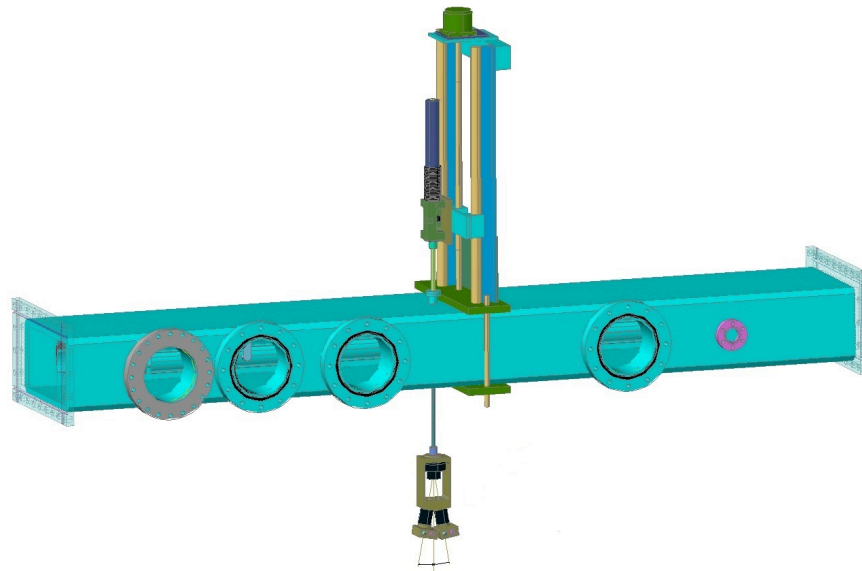
Figure 12.22: The laser is mounted above the vacuum chamber on a stage so that the laser, G10 tube and crystal can be used to measure the B-field along the vertical axis. The light from the two arms of the prism is detected with photo-diodes that are not shown.
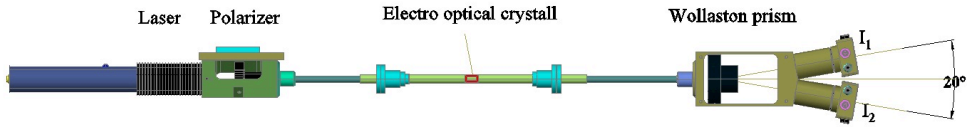
Figure 12.23: Magnetometer showing laser, polarizer, electro-optical crystall (TGG) and prism.
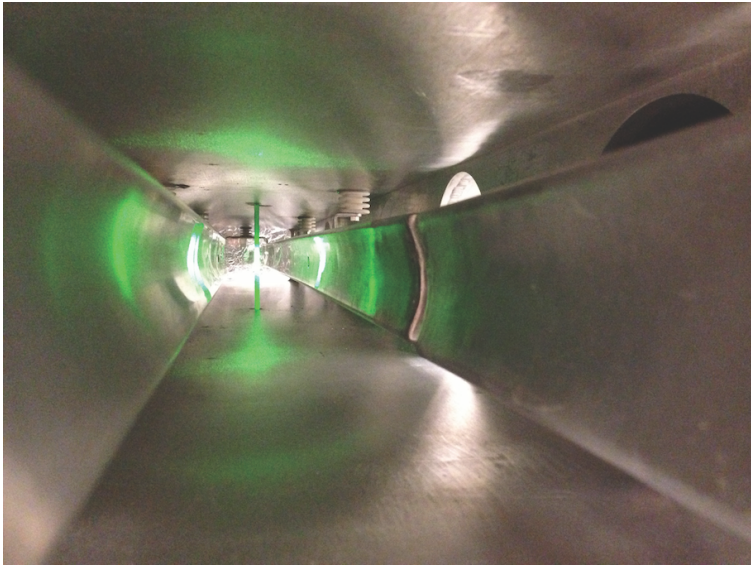
Figure 12.24: Green laser light passes through the crystal that is mounted between the kicker plates.

12.7 Risks

12.7.1 Performance Risk

The kicker system is designed to provide an integrated field of 1310 G-m for the duration of the length of the injected muon pulse ($\sim$ 120ns), and then drop to zero field, 149ns after the first muons entered the ring. Failure to achieve the specified field value will result in reduced muon capture efficiency and increased coherent betatron oscillation of the muons that are captured. Failure to turn off after 149 ns will likewise compromise capture efficiency and contribute to coherent betatron motion. The risk of less than optimal system performance are increase in statisical error (fewer muons) and additional systematic error (increased coherent betatron motion). The measured kicker current pulse is shown above 12.21(Right) and a numerical representation in Figure 12.25(Left). A tracking study quantifies the performance penalty due to the imperfect nature of the pulse shape (finite rise and fall time), and the nonuniformity of the kicker field resulting from the optimization of the plate geometry for efficiency. The study is summarized in Figure 12.25(Right). There is a negligibly small capture efficiency penalty due to the spatial non-uniformity of the kicker pulse. The effect of the finite rise and fall time, and the tail that persists beyond 149 ns, is a loss of capture efficiency of about 17%. The effort to eliminate the impedance mismatch responsible for
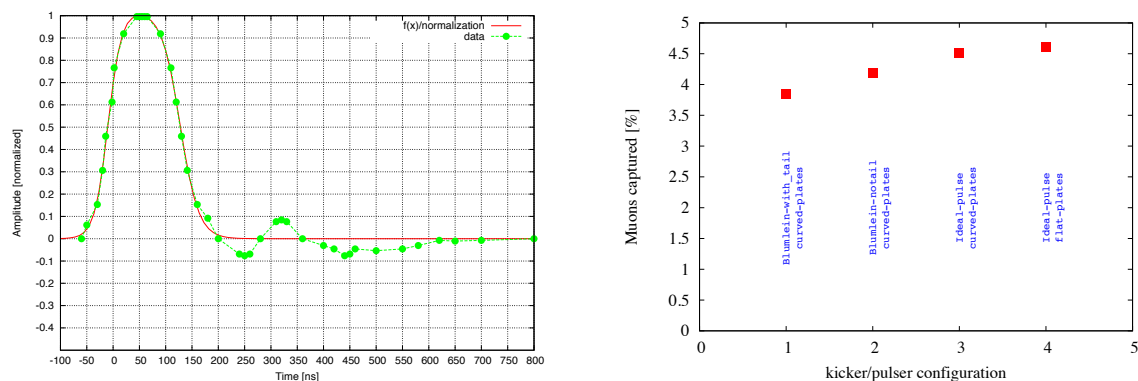
Figure 12.25: The capture efficiency for each of four kicker configurations is shown in the plot. Configuration 4-Perfect rectangular pulse shape and perfectly uniform magnetic field; 3-Perfect rectangular pulse with field profile corresponding to the curved plates; 2-Pulse shape as shown by the red curve at left; 1-Pulse shape as shown by green points and dashed green curve at left.

the tail is continuing. The source of the mismatch may be deterioration of the Blumlein transformer oil, nonstandard impedance of the cables, and/or dimensional errors in the Blumlein. An impedance transformer that includes tunable resistance and capacitance to match blumlein to cables is being developed.

As noted above, the pulse rise and fall times can be reduced, and the flat top increased, by reducing the length of the kicker plates. If necessary, a fourth kicker and Blumlein driver

could be added to increase the integrated field.

A failure of the thyratron tube, a breakdown internal to the Blumlein-PFN, or a breakdown of the plates inside the vacuum chamber would have more catastrophic consequences, as very few muons will store without an operational kicker. The risk of system failure will be mitigated by operating the kicker system continuously for a month at the design repitition rate and at voltage 10% above design to demonstrate integrity prior to installation in the ring. The current generator is designed to operate at less than 70kV, well below the level at which the E821 system was limited by breakdown.

There is some risk that the kicker will excite a long lived eddy current in the vacuum chamber that will in turn generate a lingering magnetic field that will alter the muon precession frequency. The characteristics of persistant field will be calculated and measured.

The vacuum feethrough will be cooled with Fluorinert, rather than transformer oil, so that in advent of a leak to vacuum, the storage ring vacuum system is not contaminated with oil.

The high speed switching of high voltages and currents through the stripline plates can be a significant source of electro-magnetic noise. A series of tests to determine the effect of the noise on the detector electronics will be performed and grounding scenarios to minimize its impact on the experiment identified.

12.8   Quality Assurance

The quality of the kicker system will be assured by extensive testing in advance of installation into the ring. While a single power supply and high voltage transformer has the capacity to power all three kicker/PFN system, we are planning to use independent supplies so that in the event of a high voltage problem with one of the systems, the others are unaffected.

12.9   ES& H

The kicker system will operate at high voltage $\sim$ 70kV, however there will be no exposed high voltage electrodes. All external surfaces of the Blumlein will be fixed at ground potential. As there are no diodes in the charging circuit, the time constant for dissipation of stored charge is a few seconds. A procedure for de-energizing, in order to dissipate stored energy, in the event that repair or dissassembly is required will be established. Each of the three Blumlein tri-axial lines will be filled with castor oil and an oil containment system implemented. While there is the danger of a spill, (75 liters/line), the oil itself is not hazardous.

12.10   Value management

We are reusing as much as possible, components from E821 including charging power supplies and transformers. The E821 thyratrons are not suitable and will be replaced with the higher current, lower voltage, 2 gap CX1725X thyratron.

References

[1] Efstathiadis E, et al. *Nucl. Inst. and Methods Phys. Res.* A496:8-25 (2002)

[2] A.D. Blumlein, Apparatus for Generating Electrical Impulses, U.S. Patent No. 2,496,979 Feb 7(1950).

[3] CST STUDIO SUITE, CST Computer Simulation Technology AG, www.cst.com

[4] A1A-CX1725X Issue 5, October 2002, E2V Technologies Limited 2002